Analyzing the Redox Environment of CcmK3 and CcmK4 Knockout Mutants in Cyanobacterial Carboxysomes

By Emma Snyder

University of Colorado Boulder

Department of Biochemistry

Honors Thesis Advisor: Dr. Jeffrey Cameron, Department of Biochemistry

Honors Council Representative: Dr. Halil Aydin, Department of Biochemistry

Honors Thesis Committee Outside Member: Dr. Caitlin Kelly, Department of Ecology and Evolutionary Biology

Defense Date: April 3rd, 2023

Acknowledgements

I would like to thank my thesis advisor, Dr. Jeffrey Cameron, my honors council representative, Dr. Halil Aydin, and my honors thesis committee outside member, Dr. Caitlin Kelly. I would also like to thank Clair Huffine for her extensive support and guidance throughout my project. Finally, I want to thank The Cameron Lab group for their support throughout my time in The Cameron Lab.

Table of Contents

Background

Cyanobacteria are a group of prokaryotic microorganisms that undergo photosynthesis, and contribute significantly (about 25% of all fixed carbon dioxide) to global nutrient cycles (Behrenfeld, M.J., 2001). They contain a bacterial microcompartment (BMC), the carboxysome, which aids the cell in photosynthesis by concentrating CO_2 around the carbon fixing enzyme ribulose-1,5-bisphosphate carboxylase/oxygenase (RuBisCO). The isolation of RuBisCO improves carbon fixation not only by saturating the enzyme with its preferred substrate, CO_2, but in preventing photorespiration by excluding O_2 from crossing the carboxysome shell. When RuBisCO reacts with O_2, RuBP is consumed and 2-phosphoglycolate is produced. Because 2-phosphoglycolate is not metabolically useful, the energetically expensive and inefficient process, photorespiration, must recover the lost CO_2 (Bauwe, H., 2012)(Shi, 2021). Unlike CO_2 and O_2, polar bicarbonate ions (the precursor to CO_2) and RuBP are allowed to diffuse into the carboxysome, and 3PGA diffuses out while preventing the leakage of CO_2 from the interior (Kinney, J.N., 2011)(Faulkner, M., 2020)(Figure 1).

Figure 1.

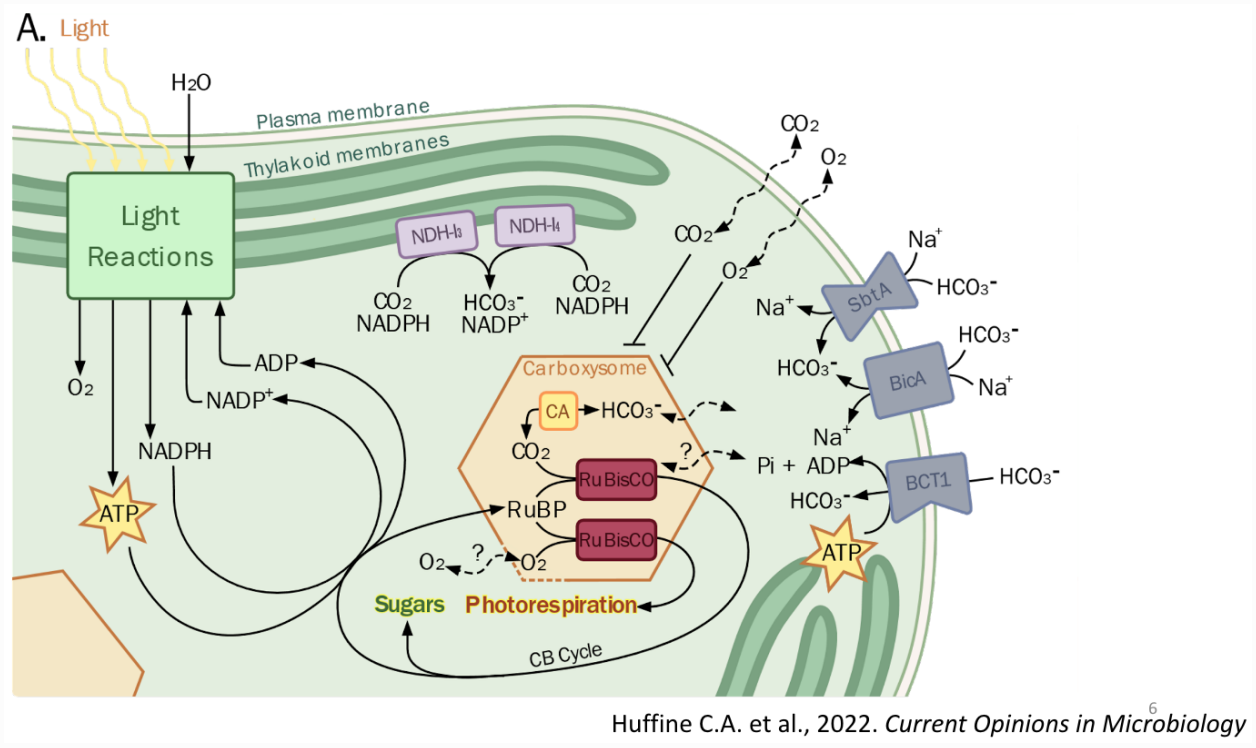

Unlike HCO_3^-, CO_2 and O_2 are unable to enter or leave the carboxysome due to its charged protein shell. Inside the carboxysome, Carbonic Anhydrase converts bicarbonate into carbon dioxide, and RuBisCO reacts with its preferred substrate, CO_2.

The carboxysome has icosahedral symmetry, and its outer shell is composed of various proteins which come together to form trimeric, pentameric, and hexameric oligomers. These oligomers each have a positively charged pore formed at their centers, which allows for the passage of the metabolites involved in carbon fixation. There are various, essential structurally determinant genes of the carboxysome shell which form its different facets, including CcmO, CcmL, and CcmK2, which have . This paper and project focus on non-essential, hexamer forming components, CcmK3 and CcmK4. Previous research has found that CcmK3 and CcmK4 are unnecessary for formation of the carboxysome, but are needed for its refined function and are

highly conserved (Rae, B. D., et al 2012). Meaning, without CcmK3 and CcmK4, cyanobacteria form physiologically stunted carboxysomes that experience slower growth rates unless incubated in high CO_2 conditions. Unlike other structural components of the carboxysome, the *ccmK3-ccmK4* genes are located on satellite loci. This could be to allow these proteins to be expressed as needed according to changing environmental conditions, as opposed to other constituently expressed shell proteins (Sommer et al 2018).

Previous research has shown that metabolic activity of cyanobacteria does not significantly decrease with deletion of either *ccmK3* or *ccmK4*. Only upon tandem deletion of these proteins is there an observed impairment to the cells' activity, suggesting that CcmK3 and CcmK4 may be functionally redundant (Rae, B. D., et al 2012, Figure 2). This is in contrast to a separate study (Sommer et al 2018), which found that deletion of *ccmK4* alone was enough to hinder the cells' growth rate because the CcmK4 protein has the ability to form hexamers with other CcmK4 proteins (homo hexamers) as well as with CcmK3 proteins (hetero hexamers). Unlike CcmK4, CcmK3 cannot form homohexamers due to steric hindrance from bulky residues, which disable formation of a permeable pore and disrupt inter-oligomer interactions. As such, CcmK3 is only observed to form CcmK4:CcmK3 heterohexamers in a ratio of 4:2. CcmK3-K4 heterohexamers have also been found to form stacks of two, dodecamers, which could serve as a way to cap and uncap carboxysome pores according to the cells needs (Sommer et al 2018, Figure 3).

For this project, we will be using *ΔccmK3-ccmK4* mutants (strains that have CcmK3 and CcmK4 proteins knocked out) and will be looking more closely at how this mutation affects the cells' and carboxysomes' redox environment, what this could mean for the carboxysome

lifecycle, and potentially gain insight as to the purpose of the CcmK3 and CcmK4 structural determinants. In general, we expect to see the redox environment of the cytosol to be more reduced than that of the internal carboxysome. We hypothesize that, in *ΔccmK3-ccmK4* mutants, the carboxysome will remain more oxidizing than the cytosol as seen in wild type cyanobacteria (Chen, A.H., 2013)(Carpenter, W.B., 2022).

Figure 2 (B. D., et al 2012)

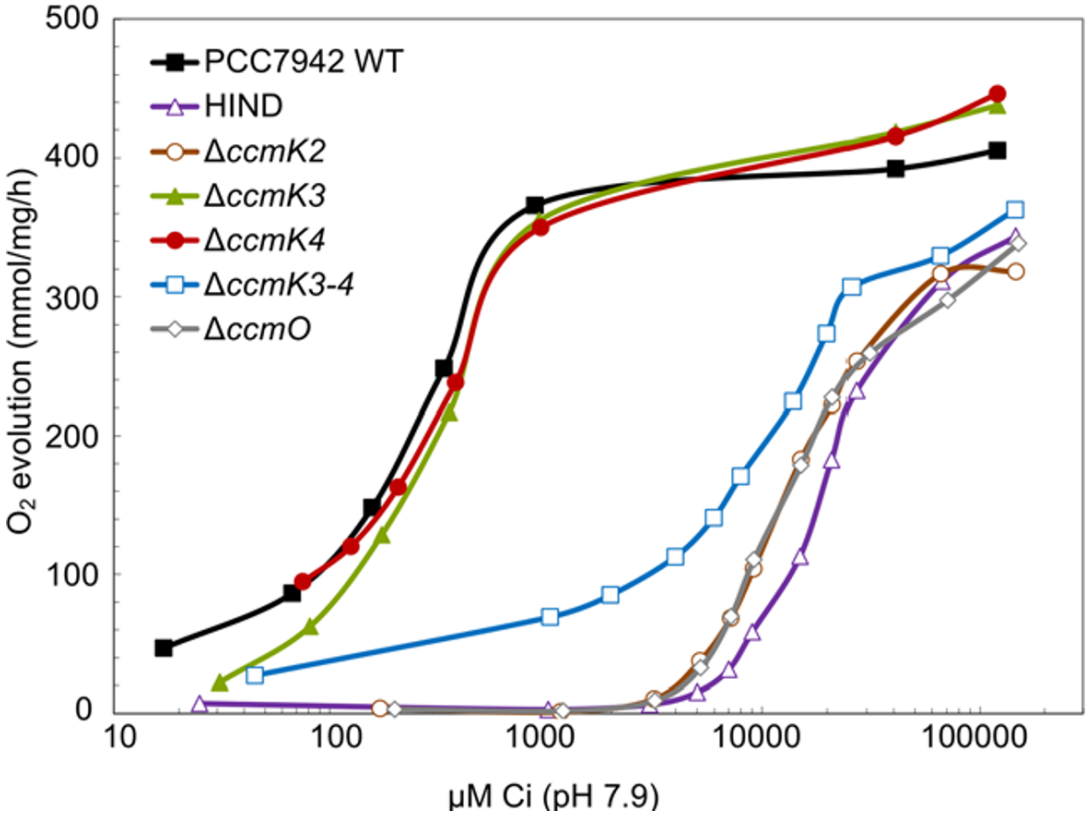

Photosynthetic oxygen evolution in response to external [Co2+HCO3-] (C_i) by BMC shell mutants.

Shown are a set of mass-spectrometric measurements of C_i-dependent O_2 evolution by wild type and mutant strains of cyanobacteria over a range of C_i concentrations. This graph shows that removing CcmK3 or CcmK4 proteins individually has little effect on metabolic activity. Only when you remove them in tandem is there a significant impairment to the cells' activity.

Figure 3 (Sommer, M. Plant Physiology 2018)

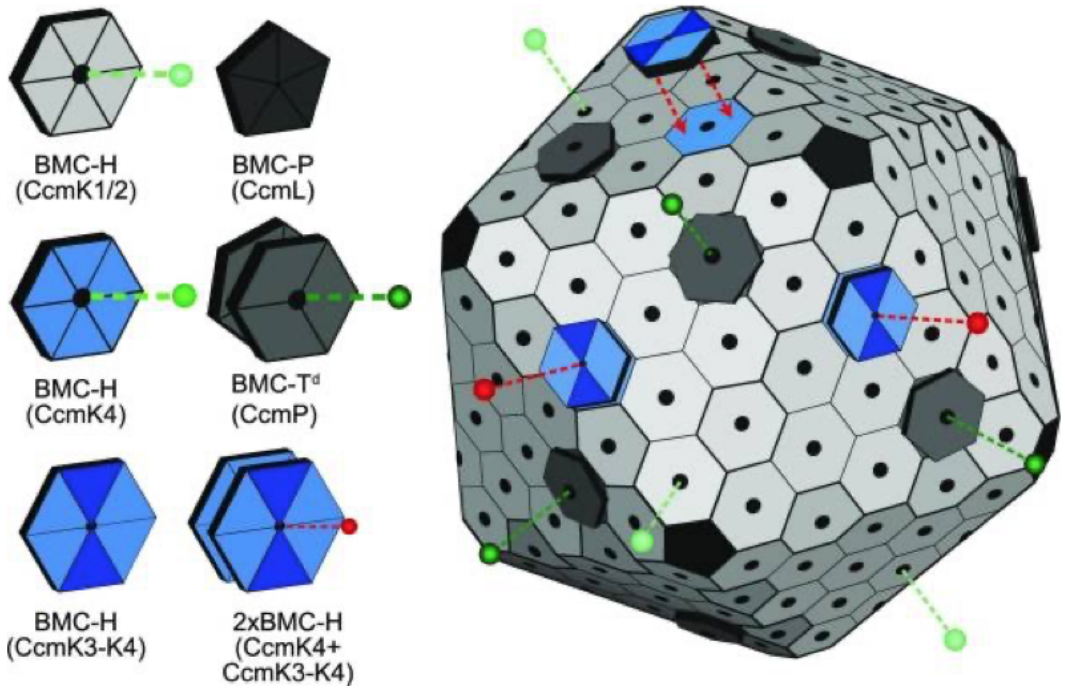

Here is a proposed model of the carboxysome which shows the essential shell proteins, as well as the CcmK3-K4 Heterohexamer formation and CcmK4 Homohexamer. In this diagram, the green dashed lines represent pore-specific metabolite flux, and the red dashed lines represent altered metabolite flux as a result of dodecamer formation between BMC-H CcmK4 and BMC-H CcmK3-K4.

Methods

We begin by creating redox sensitive green fluorescent protein (roGFP) tagged *ΔccmK3-ccmK4* mutants. Then we use widefield time lapse microscopy to film the roGFP *ΔccmK3-ccmK4* mutants, and analyze how the fluorescence of the roGFP changes over time using the MATLAB image analysis program, CyAn (Tay, J.W., Cameron, J.C., 2020). From the image analysis, we can extract quantitative information about the redox environment of the cell over the course of the film.

In order to look specifically at the redox environment of *ΔccmK3-ccmK4* mutants, we first needed to find a way to sense changes in the redox environment of wild type cyanobacteria. To do this, we created our first 'round' of mutants, which had tagged RuBisCO and cytosolic glutathione or hydrogen peroxide redox sensing green fluorescent protein (roGFPs). These roGFP proteins have been shown to be highly specific and sensitive to oxidized glutathione or hydrogen peroxide levels (Reuter, W.H., et al 2019). By comparing the intensity of roGFP fluorescence, we are able to use a ratio of emission from excitation at 395 nm and 470 nm to determine whether the environment is relatively reduced or oxidized. After inserting the roGFPs into the wild type cells, we made the second 'round' of mutants. For this second round, we removed the *ΔccmK3-ccmK4* gene, and replaced it with resistance to the antibiotic kanamycin via genetic recombination. In total, we created eight mutant strains (Figure 4).

Figure 4 (Courtesy of Clair Huffine)

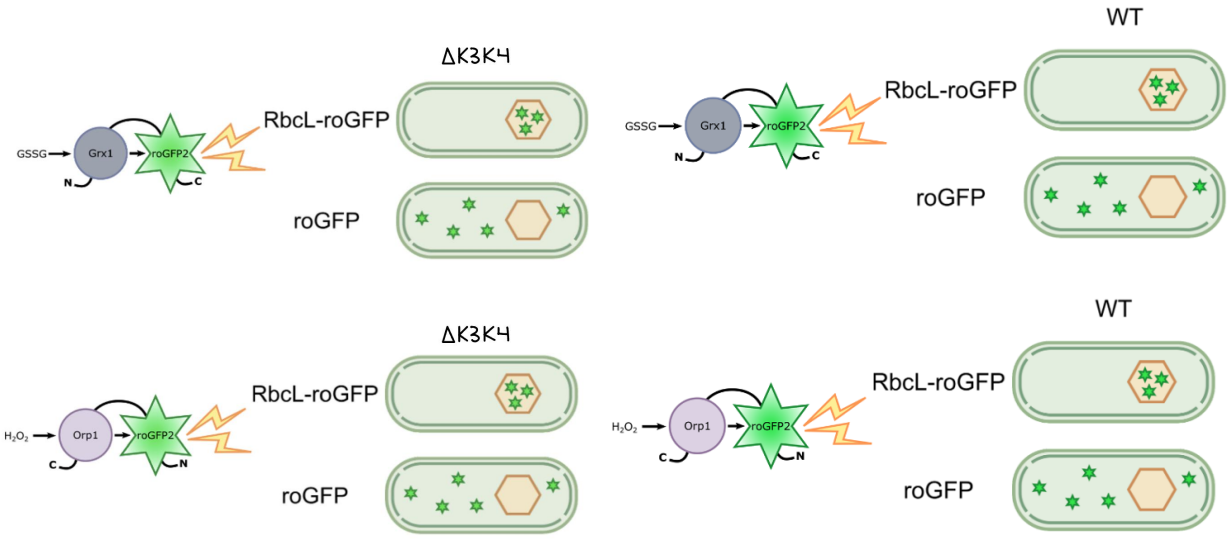

Construction of strains used in this study. The four strains on the top row contain the Grx1 (glutathione sensitive) sensors, and the bottom four contain Orp1 (hydrogen peroxide sensitive) sensors. Strains that say RbcL-roGFP

means the RuBisCO inside the carboxysome is tagged with the redox sensitive GFP system. Strains that say roGFP have the redox sensitive GFP system soluble in the cell's cytosol.

As a way to verify our strains' growth rates, their growth rates were compared to those of WT and *ΔccmK3-ccmK4* with no roGFP via dilution spot plate assays in ambient (0.03%) and elevated (3.0%) CO_2 conditions. Elevated CO_2 allows cells with mutant carboxysomes to grow normally, so on 0.5% agar plates we expect mutants to grow at the same rate as WT cells. Previous work has shown that cultures grown on 1% agar in high CO2 conditions display lower growth rates due to mechanical restriction of the cells by the agar, so we expect to see stunted growth for all cultures on 1% agar dilution spot plates (Moore, K.A., 2020).

We imaged the roGFP *ΔccmK3-ccmK4* mutants in a co-culture with wild type cells, which had been freshly grown in A+ medium and diluted to 0.05 OD at 730nm. The roGFP *ΔccmK3-ccmK4*/Wild Type cell co-culture was enclosed in a cage incubator under a mechanized inverted fluorescence microscope using the same protocol outlined in, 'Computational and Biochemical Methods to Measure the Activity of Carboxysomes and Protein Organelles in Vivo' (Tay, Cameron, 2022, Figure 5). The cells were grown for 40 hours under a constant growth light, and were imaged using lasers to excite fluorescence every twenty minutes. We used excitation wavelengths of 650 nm to excite chlorophyll, and 395 nm/470 nm to excite the roGFP.

Figure 5 (Tay, JW. Cameron, JC. Methods in Enzymology, 2022)

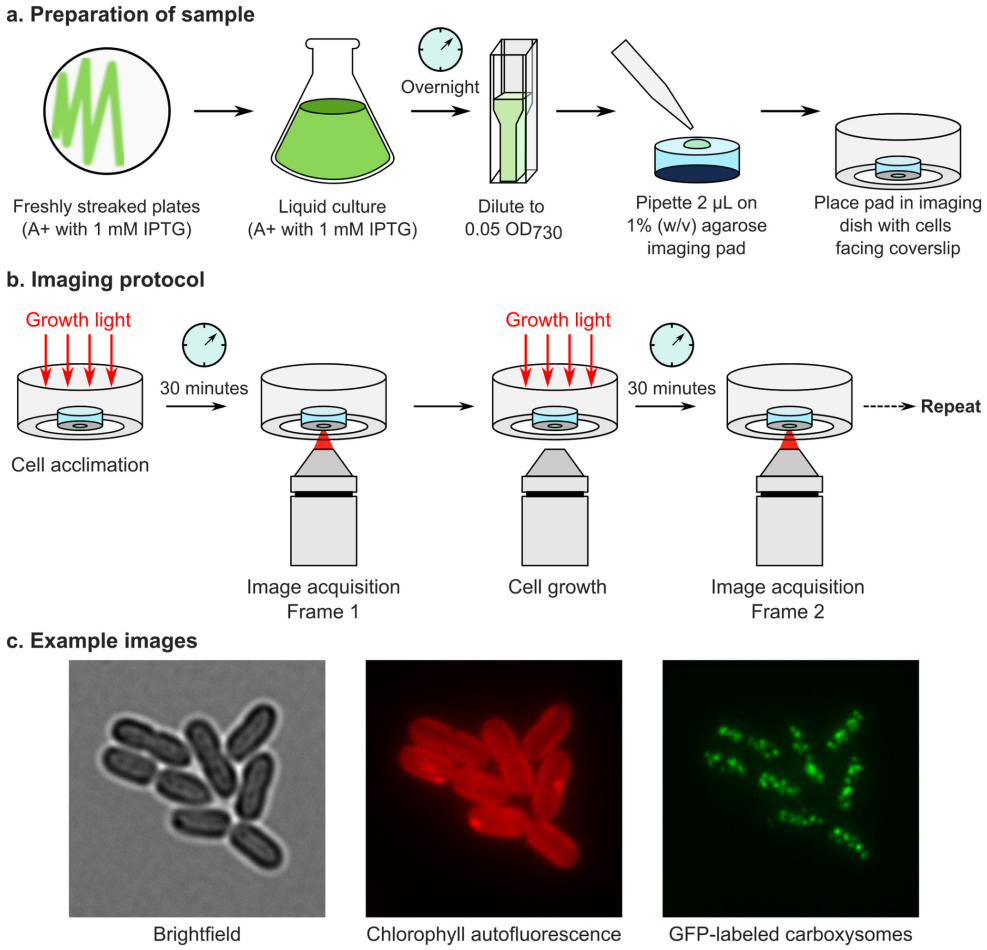

Sample preparation and standard imaging protocol. (a) Protocol showing preparation of the sample. (b) Schematic showing a typical imaging protocol. Note: in this study, we imaged cells every twenty minutes instead of every thirty minutes. (c) Example images of cyanobacteria under different excitation wavelengths, showing the brightfield image, chlorophyll fluorescence, and GFP-labeled carboxysomes.

Once the timelapse images had been gathered, we used the image analysis program, CyAn, to extract numerical data on fluorescence intensities and cell size from the images. CyAn auto generates a cell mask overlay that tracks cell size by assigning each pixel to one cell over the course of the movie. Once the time lapse mask is auto generated, the mask of each time lapse frame is hand corrected for any mistakes, and the final cell mask is produced. Using this cell

tracking system, to identify carboxysome puncta within individual cells, we can calculate ratiometric values for the redox states within each carboxysome and cell (Figure 6).

Figure 6 (Courtesy of Clair Huffine)

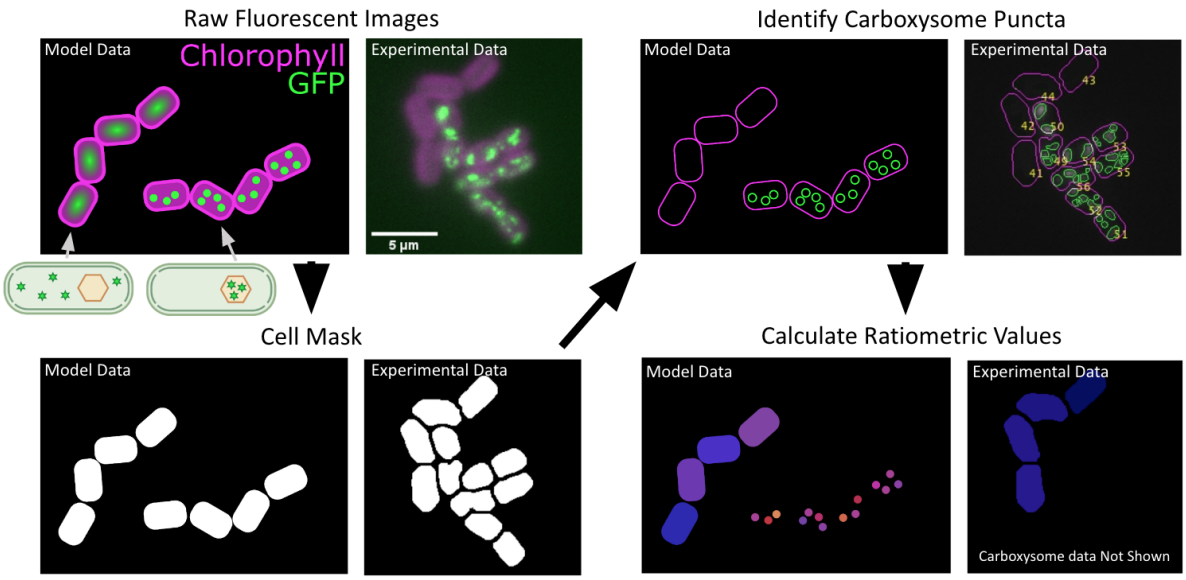

We start with raw fluorescent images from the timelapse. Then, MATLAB image processing toolbox, CyAn, generates a cell mask which is then hand corrected frame by frame. From this cell mask, CyAn assigns numbers to each cell and carboxysome, and generates a ratiometric color value for the redox environment of each cell per frame.

Results

The first few times we tried to confirm that we had isolated the proper strains using PCRs and chromosome extractions, the gel electrophoresis did not display any bands. To work around this, we decided to make new primers which had a smaller range in melting temperatures, and were located at slightly more favorable base pairs for the PCR. The new primers worked, and we were able to use gel electrophoresis to confirm our mutant strains (Figure 7). Since we replaced the *ccmK3-ccmK4* sequence with Kanamycin resistance, the top reaction used primers for the

sequence containing Kanamycin resistance, which was about 802 base pairs long. We included the wild type cyanobacteria as a negative control and purified *ΔccmK3-ccmK4 (Kanamycin Resistance)* plasmid as a positive control. On the gel, we see bands at the proper size for three out of four mutant strains. In the first column, however, there is no band. We discovered that the carboxysome labeled glutaredoxin sensing strain (ΔCcmK3-CcmK4 RbcL-Grx1-roGFP) had stopped working, likely due to a random mutation (Figure 8). Because one strain of the Grx-1-roGFP mutants stopped working, we imaged the hydrogen peroxide sensitive, Orp-1-roGFP pair, instead.

Figure 7

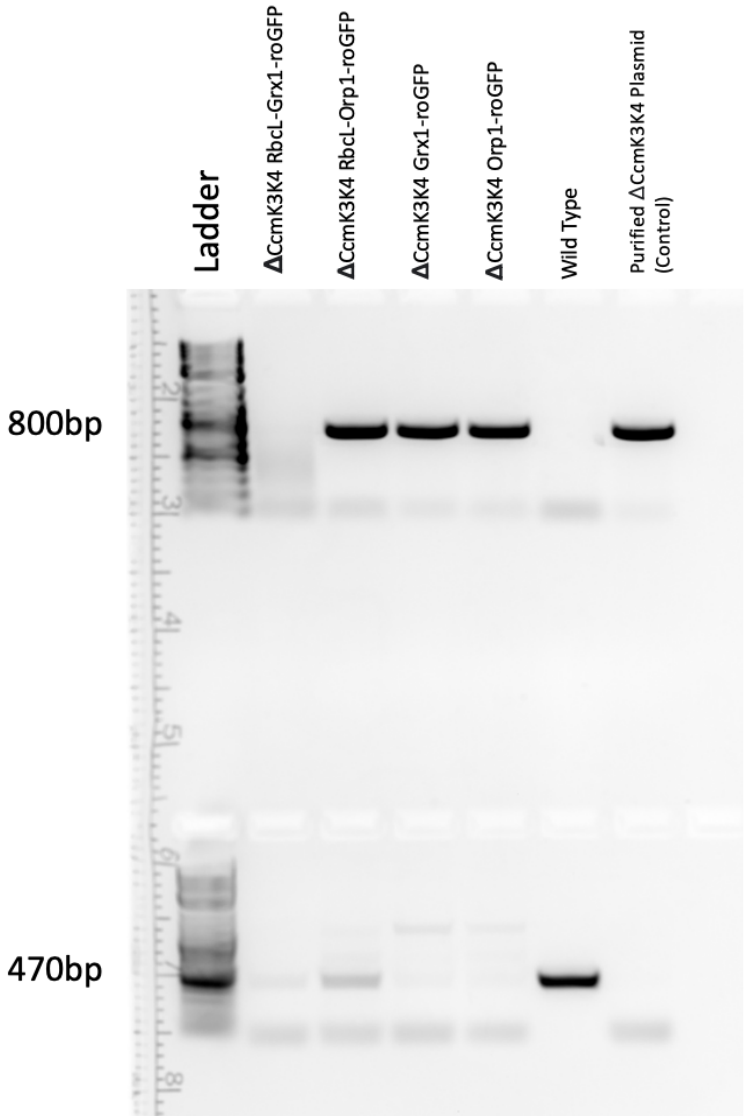

PCR and Gel Electrophoresis show which mutants have the correct sequences. The top bands show the isolated plasmids from a PCR using primers for the sequence containing the Kanamycin resistance we replaced CcmK3-K4 with. Three strains show expected bands (~806 base pairs) to confirm that they contain Kanamycin resistance. (*ΔccmK3-ccmK4*) The carboxysome labeled Grx1-roGFP does not have a band for Kanamycin resistance. The bottom bands show a PCR using primers for a sequence containing CcmK3-K4. Since we removed *ccmK3-ccmK4,* we expected to see no bands for our mutant strains, which is what is shown. Since the carboxysome labeled

Grx1-roGFP does not have a band here, it suggests that the mutation occurred in the Kanamycin resistance sequence.

Figure 8

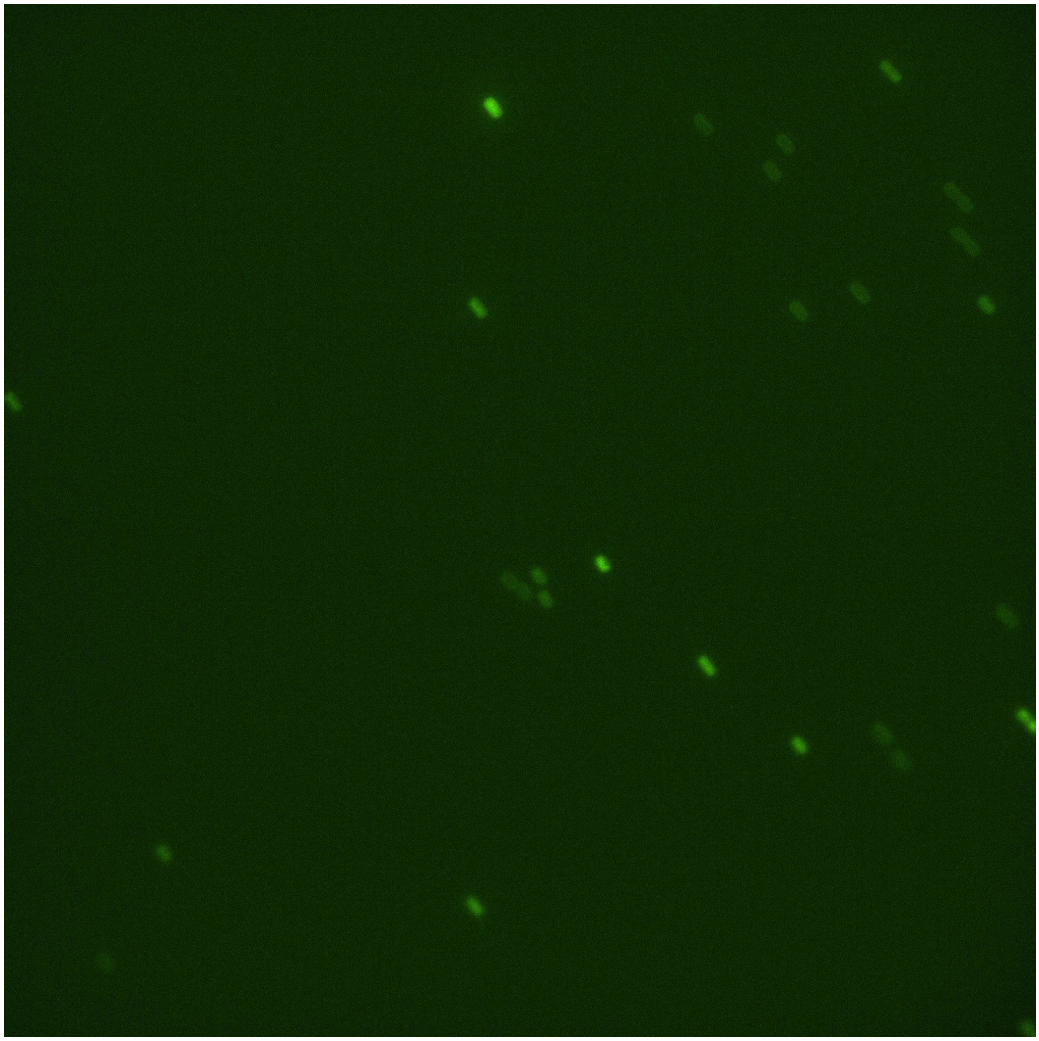

This is a co-culture of the carboxysome and cytosol labeled Grx1 sensor mutants. The image clearly shows that the carboxysome labeled strain does not contain green fluorescent protein.

To get a qualitative view of the *ΔccmK3-ccmK4* strains' relative growth rates, we created spot plates of each strain on 1.0% and 0.5% agar plates, using A+ medium to dilute each column by 0.1% (Figure 9). Each plate was incubated in either high CO_2 (3%) or air (0.04%) conditions.

Cultures grown on 0.5% agar in air seem to have almost equal growth to the cultures grown on 0.5% agar in high CO_2. Since *ΔccmK3-ccmK4* strains are known to be physiologically impaired unless in CO_2, we expected to see lower growth rates in air on the 0.5% agar plates. In general, the cultures grown on 1% agar in air show higher growth rates than those grown at high CO_2, as anticipated. However, the Orp-1 roGFP containing strains grown on 1% agar in high CO_2 are able to grow despite the mechanical restriction of the 1% agar. This difference could be due to some advantage provided by having the roGFPs reacting with GSSG and hydrogen peroxide to help reduce oxidative damage to the cell.

Figure 9

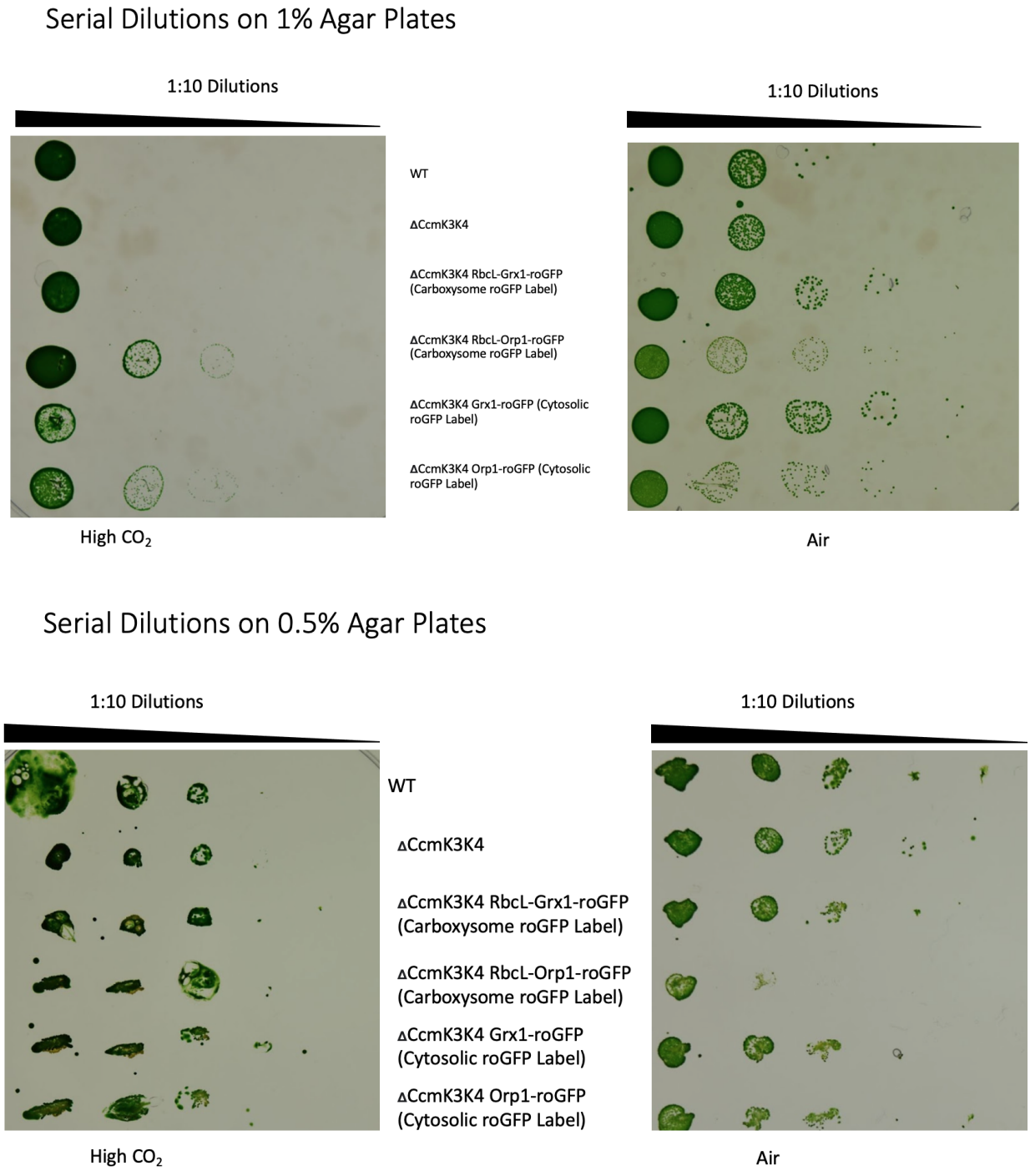

Once we had created and confirmed our *ΔccmK3-ccmK4* Orp-1-roGFP strains, we moved on to bulk characterization of the pair to validate that the fluorescent proteins were reacting to

oxidizing and reducing agents in the expected manner. To begin this process, we performed a chlorophyll normalization on samples of wildtype, *ΔccmK3-ccmK4* Orp-1-roGFP (cytosolic roGFP strain), and *ΔccmK3-ccmK4* RbcL-Orp1-roGFP (RuBisCO tagged roGFP strain), and diluted them to OD 0.3 at 730nm. We then ran excitation scans on a spectrofluorometer on each strain after the addition of oxidizing and reducing agents, Dithiothreitol and Hydrogen Peroxide. The excitation scans (Figure 10) showed that neither mutant produced a fluorescence above the WT baseline at 390nm, and only the carboxysome labeled strain produced a significant signal at 470 nm. This eliminated the possibility of extracting redox data from the strain with roGFP-Orp1 in the cell cytosol. We were able to obtain data, however, on the redox environment of the carboxysome labeled RbcL-roGFP-Orp1 strain (Figure 11). The data produced shows that the redox state of the internal carboxysome remains relatively stable throughout the timelapse.

Figure 10

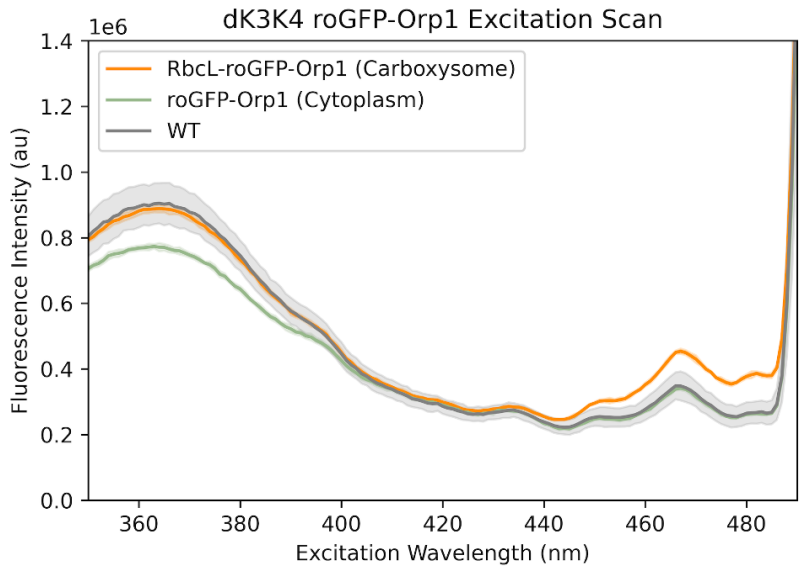

The fluorescence intensity of roGFP-Orp1 (Cytoplasm) is below the wild type baseline at 395 nm and 470 nm. The RbcL-roGFP-Orp1 (Carboxysome) fluorescence intensity is about equal to wild type at 395 nm and above wild type at 470 nm.

Figure 11

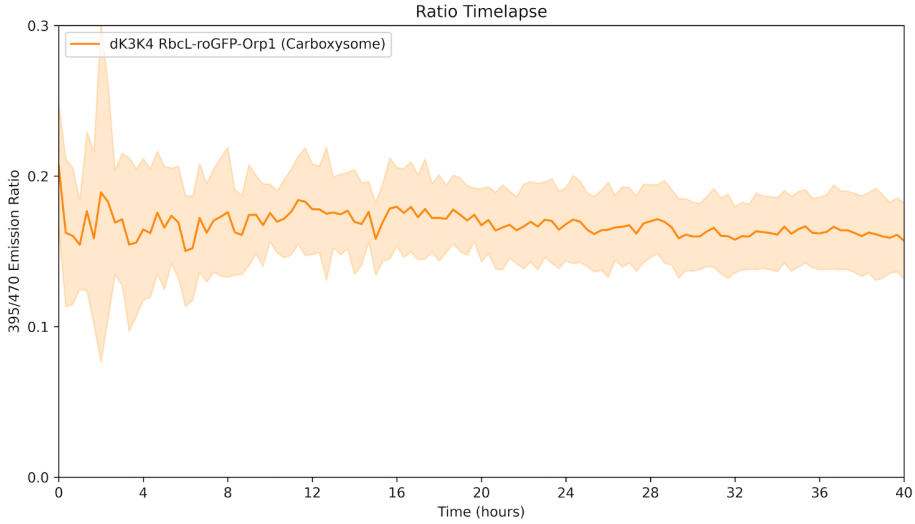

This graph shows how the fluorescence intensity ratios of the RbcL-roGFP-Orp1 (carboxysome) strain changes every twenty minutes. The redox of the internal carboxysome seems to be relatively constant, however, it should be noted that this data was obtained from a mutant strain that was not confirmed to be fluorescing at intensity above baseline.

Despite this setback, we were still able to get some interesting images of the *ΔccmK3-ccmK4* RbcL-Orp1-roGFP (RuBisCO tagged roGFP strain). The images in Figure 12 are of one colony of this strain captured under excitation wavelengths for chlorophyll and roGFP, then overlaid onto each other in the center image. In some cells, there seems to be an association between the chlorophyll and carboxysomes. This membrane association has previously been shown to occur in defective carboxysomes, which could be what is happening in the images from Figure 12 (Cameron, J.C., 2013).

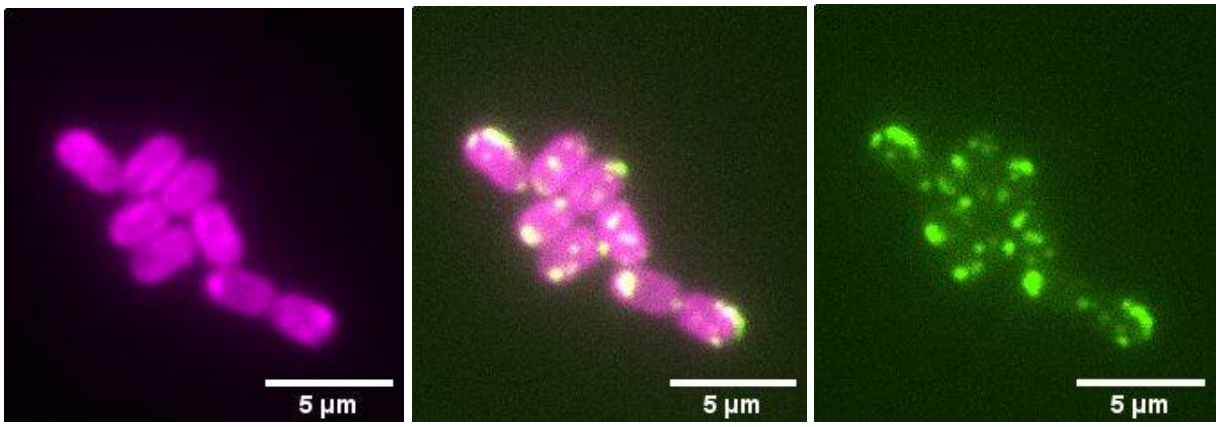

Figure 12.

All three images show the same frame of the same colony under different excitation wavelengths. The image on the far left shows chlorophyll in magenta. The image on the far right shows the RuBisCO tagged roGFP (carboxysome). The center image shows the overlay of the two images. Some cells appear to have an association between the chlorophyll and carboxysomes.

Discussion

The results from Figure 9 of our project further support previous research suggesting that CcmK3-K4 is non-essential to carboxysome formation. Our spot plates show that mutant cells lacking CcmK3 and CcmK4 heterohexamers grow both at high CO_2 conditions and in air, whereas carboxysome mutants lacking other essential structural proteins (like CcmK2 and CcmO) are unable to grow outside of high CO_2 incubation. We know from previous research, as discussed in the methods section, that cultures grown on 1% agar plates in elevated (3%) CO_2 are expected to display stunted growth rates as a result of mechanical restriction by the agar (Moore, K.A., 2020). This is displayed in Figure 9 of the Results section. Unexpectedly, the growth rates on the 1% agar plates displayed in Figure 9 also show that the Orp-1 roGFP tagged mutants are able to grow in high CO_2 incubation, which is not what prior research would predict. One

potential explanation for this could be that the Orp-1 roGFP sensor system helps combat oxidative cell damage that occurs in *ΔccmK3-ccmK4* mutants via the Orp-1's reduction of hydrogen peroxide. The overall decrease in concentration of this oxidizing molecule could give cells an advantage by decreasing oxidative cell damage.

There is still much that is not understood about the functions of the carboxysome shell protein components, CcmK3 and CcmK4. The next step of this project would be to fix the mutation that occurred in the Grx1-roGFP mutants and make a timelapse film using the same methods we used for the Orp1-roGFP strains. Since the Grx1-roGFP mutants are typically higher in fluorescence intensity, it is likely that the redox data obtained from this film would be insightful.

While this project has focused on the redox of CcmK3-CcmK4 tandem deletion, it would be useful to see how the cell redox is affected by single deletions of either CcmK3 or CcmK4, as discussed in the background section. This seems to be a natural next step for this project, as we would be able to start with the roGFP mutants we have already made and remove CcmK3 or CcmK4 from there.

Bibliography

Shi, Xiaoxiao, and Arnold Bloom. “Photorespiration: The Futile Cycle?” *Plants* 10, no. 5 (May 2021): 908. https://doi.org/10.3390/plants10050908.

Bauwe, Hermann, Martin Hagemann, Ramona Kern, and Stefan Timm. “Photorespiration Has a Dual Origin and Manifold Links to Central Metabolism.” *Current Opinion in Plant Biology* 15, no. 3 (June 1, 2012): 269–75. https://doi.org/10.1016/j.pbi.2012.01.008.

Carpenter, William B., Abhijit A. Lavania, Julia S. Borden, Luke M. Oltrogge, Davis Perez, Peter D. Dahlberg, David F. Savage, and W. E. Moerner. “Ratiometric Sensing of Redox Environments Inside Individual Carboxysomes Trapped in Solution.” *The Journal of Physical Chemistry Letters* 13, no. 20 (May 26, 2022): 4455–62. https://doi.org/10.1021/acs.jpclett.2c00782.

Behrenfeld, Michael J., James T. Randerson, Charles R. McClain, Gene C. Feldman, Sietse O. Los, Compton J. Tucker, Paul G. Falkowski, et al. “Biospheric Primary Production During an ENSO Transition.” *Science* 291, no. 5513 (March 30, 2001): 2594–97. https://doi.org/10.1126/science.1055071.

Faulkner, Matthew, István Szabó, Samantha L. Weetman, Francois Sicard, Roland G. Huber, Peter J. Bond, Edina Rosta, and Lu-Ning Liu. “Molecular Simulations Unravel the Molecular Principles That Mediate Selective Permeability of Carboxysome Shell Protein.” *Scientific Reports* 10, no. 1 (October 15, 2020): 17501. https://doi.org/10.1038/s41598-020-74536-5.

Cameron, Jeffrey C., Steven C. Wilson, Susan L. Bernstein, and Cheryl A. Kerfeld. “Biogenesis of a Bacterial Organelle: The Carboxysome Assembly Pathway.” *Cell* 155, no. 5 (November 21, 2013): 1131–40. https://doi.org/10.1016/j.cell.2013.10.044.

Chen, Anna H., Avi Robinson-Mosher, David F. Savage, Pamela A. Silver, and Jessica K. Polka. “The Bacterial Carbon-Fixing Organelle Is Formed by Shell Envelopment of Preassembled Cargo.” *PLoS ONE* 8, no. 9 (September 4, 2013): e76127. https://doi.org/10.1371/journal.pone.0076127.

Huffine, Clair A, Lucas C Wheeler, Boswell Wing, and Jeffrey C Cameron. “Computational Modeling and Evolutionary Implications of Biochemical Reactions in Bacterial Microcompartments.” *Current Opinion in Microbiology* 65 (February 1, 2022): 15–23. https://doi.org/10.1016/j.mib.2021.10.001.

Kinney, James N., Seth D. Axen, and Cheryl A. Kerfeld. “Comparative Analysis of Carboxysome Shell Proteins.” *Photosynthesis Research* 109, no. 1 (September 1, 2011): 21–32. https://doi.org/10.1007/s11120-011-9624-6.

Rae, Benjamin D., Benedict M. Long, Murray R. Badger, and G. Dean Price. “Structural Determinants of the Outer Shell of β-Carboxysomes in Synechococcus Elongatus PCC 7942: Roles for CcmK2, K3-K4, CcmO, and CcmL.” *PLOS ONE* 7, no. 8 (August 22, 2012): e43871. https://doi.org/10.1371/journal.pone.0043871.

Tay, Jian Wei, and Jeffrey C. Cameron. “Computational and Biochemical Methods to Measure the Activity of Carboxysomes and Protein Organelles in Vivo.” Methods in Enzymology. Academic Press, 2022. https://doi.org/10.1016/bs.mie.2022.09.010.

Tay, Jian Wei, and Jeffrey C. Cameron. “CyAn: A MATLAB Toolbox for Image and Data Analysis of Cyanobacteria.” bioRxiv, July 28, 2020. https://doi.org/10.1101/2020.07.28.225219.

Sommer, Manuel, Markus Sutter, Sayan Gupta, Henning Kirst, Aiko Turmo, Sigal Lechno-Yossef, Rodney L. Burton, et al. “Heterohexamers Formed by CcmK3 and CcmK4 Increase the Complexity of Beta Carboxysome Shells.” *Plant Physiology* 179, no. 1 (January 2019): 156–67. https://doi.org/10.1104/pp.18.01190.

Reuter, Wilhad Hans, Thorsten Masuch, Na Ke, Marine Lenon, Meytal Radzinski, Vu Van Loi, Guoping Ren, et al. “Utilizing Redox-Sensitive GFP Fusions to Detect in Vivo Redox Changes in a Genetically Engineered Prokaryote.” *Redox Biology* 26 (September 1, 2019): 101280. https://doi.org/10.1016/j.redox.2019.101280.

Moore, Kristin A., Sabina Altus, Jian W. Tay, Janet B. Meehl, Evan B. Johnson, David M. Bortz, and Jeffrey C. Cameron. “Mechanical Regulation of Photosynthesis in Cyanobacteria.” *Nature Microbiology* 5, no. 5 (May 2020): 757–67. https://doi.org/10.1038/s41564-020-0684-2.